The Effect of Droplet Size Distribution on the Determination of Cloud Droplet Effective Radius

F.-L. Chang and Z. Li
ESSIC/Department of Meteorology
University of Maryland
College Park, Maryland

F.-L. Chang
Canada Centre for Remote Sensing
Ottawa, Ontario, Canada

Introduction

Cloud microphysical processes can provide links between cloud radiative effect and hydrological cycle and create several feedback mechanisms linking clouds and climate. For instance, the aerosols can affect the climate through their indirect effect on clouds, which modifies cloud microphysical properties and hence cloud radiative properties, proving an increase in cloud albedo and a net radiative cooling (Twomey et al. 1984; Charlson et al. 1992). The key microphysical parameters affecting both radiation budget and hydrological cycle like cloud liquid water content (w) and droplet effective radius (r_e) are generally determined by the specification of cloud droplet size distribution, i.e.,

$$w = \int \frac{4}{3} \rho_w \pi r^3 n(r) dr, \tag{1}$$

$$r_e = \frac{\int \pi r^3 n(r) dr}{\int \pi r^2 n(r) dr}, \tag{2}$$

where ρ_w is the density of water, r is the droplet radius, and n(r)dr is the volume number density of the droplets with radius between r and r+dr.

Accurate determination of cloud microphysical properties is essential for the correct treatment of clouds in radiative transfer calculations and climate modeling. This study examines firstly the effect of the spectral dispersion (σ) of cloud droplet size distribution on the parameterization relationship between r_e, w, and the total droplet number concentration (N), commonly used in climate modeling. The second is to examine the effect of the spectral dispersion on the retrievals of r_e from remote sensing measurements like satellite observations. Operational satellite retrieval techniques often rely on a prior assumption of cloud droplet size distribution to invert reflectance measurements into r_e. For stratus and stratocumulus clouds, two commonly employed droplet size distributions, i.e., the lognormal and standard gamma distributions, are used here to estimate the uncertainty in r_e retrievals with various spectral dispersions.

Also, the effects of the droplet size distribution on the retrievals of r_e are compared among retrievals made from using different near-infrared (NIR) channels, i.e., 1.24, 1.65, 2.15, and 3.75 μm, respectively.

Theorectical Droplet Size Distributions

In cloud modeling and radiative transfer calculations, cloud droplet size spectra are usually characterized by the lognormal or gamma distributions. The two theoretical distributions are chosen because they adhere more closely to the droplet size spectra measured by the in situ probes during many stratus and stratocumulus observation campaigns. The lognormal size distribution is defined by

$$n_{log}(r) = \frac{N}{\sqrt{2\pi}\sigma_{log} r} \exp[-(\ln r - \ln r_0)^2 / 2\sigma_{log}^2], \quad (3)$$

where σ_{log} is the logarithmic width of the distribution as it characterizes the radius spectral dispersion, $N = \int n(r)dr$ is the total droplet concentration per unit volume, and r_0 is the median radius. The r_e for the lognormal distribution is given by

$$r_e = r_0 \exp(5\sigma_{log}^2 / 2), \quad (4)$$

The standard gamma distribution used here is defined by

$$n_{gam}(r) = \frac{N}{\Gamma[(1-2b)/b]} \frac{r^{(1-3b)/b} e^{-r/(ab)}}{(ab)^{(1-2b)/b}}, \quad (5)$$

where $a = r_e$ denotes the r_e, $b = \sigma^2_{gam}$ denotes the spectral dispersion, and Γ is the gamma function.

Relationship Between r_e, w, and N

In many cloud and climate studies, droplet r_e is determined based on the parameterization relationship given by

$$r_e = c(w/N)^d \quad (6)$$

where c and d are constants, generally determined by empirical fitting to the in situ observations at local cloud experiments (e.g., Martin et al. 1994; Liu and Daum 2000). In principle, the relationship between r_e and w/N can be derived from Eqs. (1) and (2), which is given by

$$r_e = \left[\frac{4}{3}\pi\rho_w \frac{\int r^2 n(r)dr}{\int n(r)dr}\right]^{-1} \frac{w}{N} \quad (7)$$

Figure 1 plots the theoretical relationships derived based on the lognormal and standard gamma distributions with σ_{log} and σ_{gam} set equal to 0.17, 0.35, and 0.53, respectively. Since d is commonly set to be 1/3 (e.g., Liu and Hallett 1997), Figure 1b shows the relationship between r_e and $(w/N)^{1/3}$. The corresponding values of c were derived and given in Table 1 for various spectral dispersions of the droplet size distributions. As seen from the figure, r_e differs by about 4 μm due to a change from $\sigma_{log} = 0.17$ to 0.53 for a fixed $(w/N)^{1/3}$ near 0.15. Some observations of r_e, w, and N from different marine stratocumulus experiments taken from Miles et al. (2000) were also plotted in Figure 1b. The observations generally fall within the range between $\sigma_{log} = 0.17$ and 0.53.

Table 1. Corresponding constant values of *c* derived for d = 1/3.

	s_{log} or s_{gam}		
	0.17	0.35	0.53
Lognormal	63.854	70.117	82.118
Standard gamma	63.900	71.161	91.154

The Dependence of r_e Retrieval on Spectral Dispersion

Most climate studies incorporate the droplet size information from local experiments. To extend our knowledge from small-scale cloud microphysics to large-scale cloud radiative effects thus requires operational satellite observations. Satellite measurements, for example, at 3.75 μm from the Advanced Very High Resolution Radiometer (AVHRR) and at 1.24, 1.65, 2.15, and 3.75 μm from the Moderate-Resolution Imaging Spectroradiometer (MODIS) have received widespread attention for purposes of retrieving r_e from space. The retrieval of r_e from space is established because solar reflectance in the NIR window channel has a large dependence on cloud droplet size distributions. Since measuring w and N from remote sensing are seemingly impossible, the r_e retrieval techniques rely upon a priori assumption on the droplet size distribution with constant spectral dispersion (e.g., $\sigma_{log} = 0.35$).

Figure 2 shows the dependence of the NIR reflectance on both r_e and σ_{log} for the lognormal size distribution. The figure shows for a) nadir, b) forward, and c) backward viewing directions with solar zenith angle $\theta_0 = 60°$ for cloud visible optical depth 20 at 1.24, 1.65, 2.15, and 3.75 μm. Since larger droplets absorb more solar radiation than do smaller droplets, the NIR reflectance generally has an inverse relationship with r_e. For constant r_e, the NIR reflectance also displays some variations with changes in σ_{log}. The NIR reflectance generally has a smaller dependence on σ_{log} in nadir viewing direction than in the forward or backward scattering direction. To quantify the uncertainty in the r_e retrievals by assuming a constant σ_{log}, reflectance measurements were simulated for various $\sigma_{log} = 0.17$, 0.26, 0.35, 0.44, and 0.53, respectively, with fixed r_e. Then, r_e were retrieved from these simulated reflectances by employing the lookup-table technique (e.g., Han et al. 1994), which were created by assuming constant σ_{log} of 0.35. Figure 3 shows the difference between the retrieved r_e and its original input as a function of various input r_e values for the retrievals made at nadir viewing angle with $\theta_0 = 60°$ and $12 < \tau < 20$. The figure shows the retrievals obtained for the lognormal (solid curves) and standard gamma (dotted curves) distributions, respectively. The magnitudes of the r_e differences are similar for the two distributions, which is generally on the order of ±1 μm for an input $r_e = 10$ μm. The r_e difference generally increases with increasing r_e and has the largest increase at 3.75 μm. The r_e difference is also dependent on the viewing and sun illumination geometry.

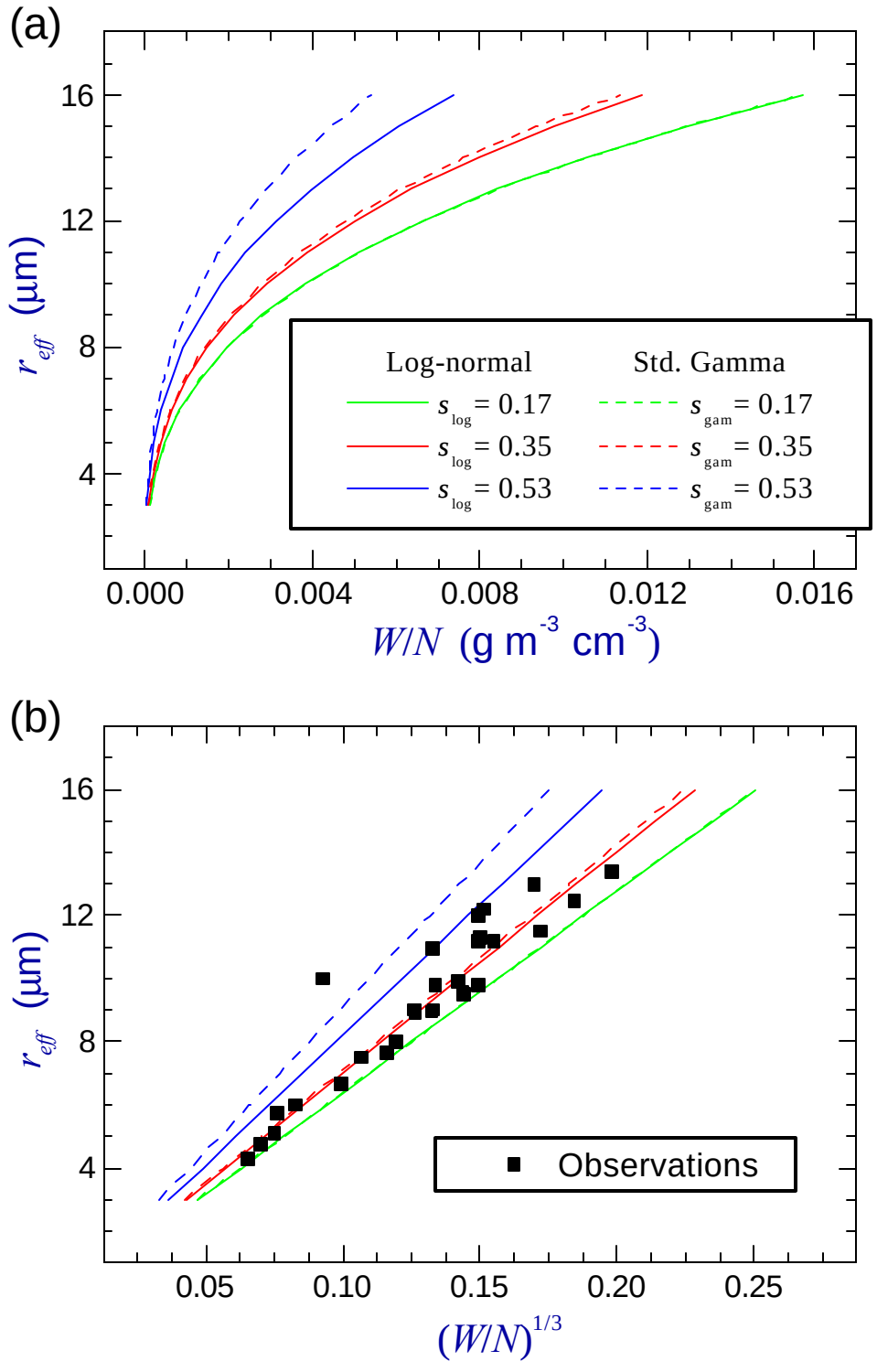

Figure 1. Theoretical relationship between (a) re and w/N and b) re and (w/N)1/3 obtained based on the lognormal (solid curves) and standard gamma (dashed curves) distributions for various size spectral dispersions. Some observations as described in the text are also plotted in (b).

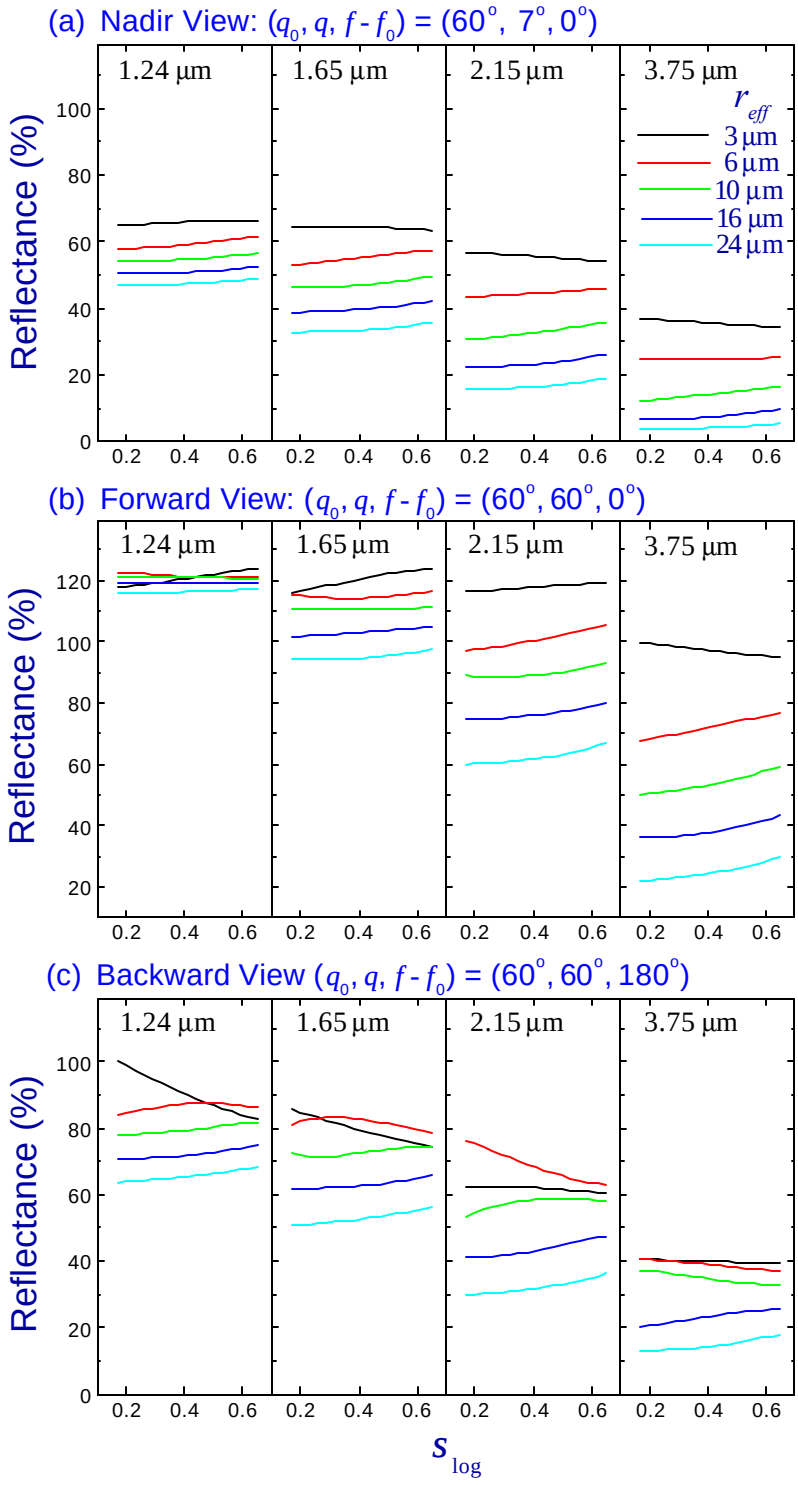

Figure 2. The dependence of NIR reflectances at 1.24, 1.65, 2.15, and 3.75 mm on slog for (a) nadir, (b) forward, and (c) backward viewing directions. Results are shown for constant re = 3, 6, 10, 16, and 24 mm with a cloud optical depth of 20.

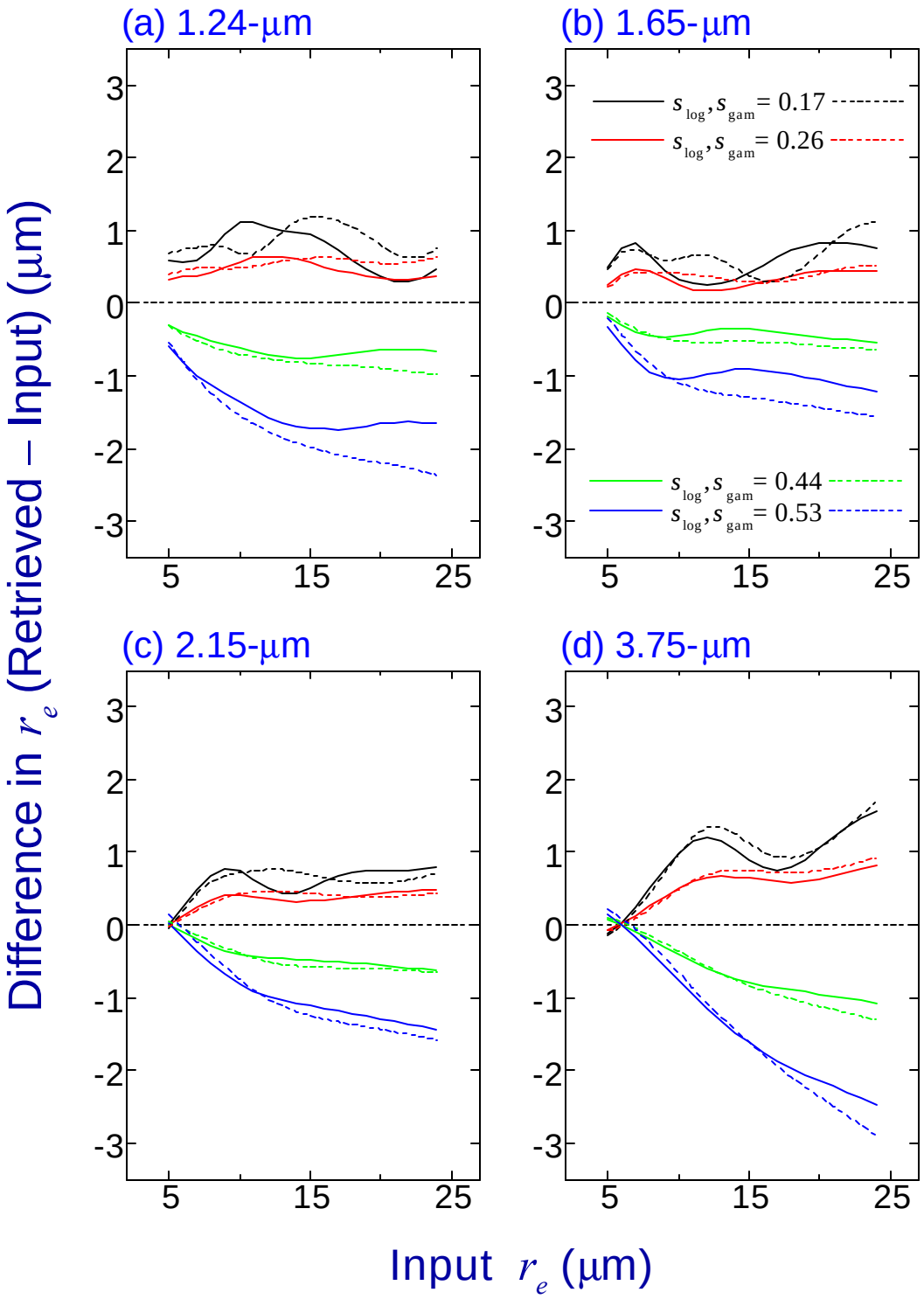

Figure 3. The dependence of the difference between the retrieved and input re on the input spectral dispersion (s) plotted as a function of the input re for (a) 1.24, (b) 1.65, (c) 2.15, and (d) 3.75 mm. The solid curves were derived based on the lognormal distribution with various input of slog; likewise, the dashed curves were derived based on the standard gamma distribution.

Summary

This study examines the impact of droplet size distribution on the relationship between r_e, w, and N and the sensitivity of remote sensing retrieved r_e to different a priori assumptions of the droplet size spectral dispersion. The determination of r_e, based on w and N, is found to be dependent on the droplet size distribution and its size spectral dispersion. Even with constant w and N, the determination of r_e may vary by a few microns with changes of σ_{log} from 0.17 to 0.53 for a lognormal distribution. The remote sensing determination of r_e, based on NIR reflectance measurements, is also dependent on the droplet size distribution. The dependence is generally smaller at near nadir viewing angles than at forward or backward scattering directions. With the lognormal size distribution, a change of ±0.15 in spectral dispersion from σ_{log} = 0.35 may lead to a change of about ±1 μm in the mean of the r_e retrievals at around 10 μm. The change increases as r_e increases. Further studies, based on observational spectral dispersions of the droplet size distributions, are needed to quantify their effects on the determination of r_e.

Acknowledgement

This work was supported by the U.S. Department of Energy Grant DE-FG02-97ER62361 under the Atmospheric Radiation Measurement (ARM) Program.

Corresponding Author

Dr. Zhanquing Li, zli@atmos.umd.edu, (301) 405-6699

References

Charlson, R. J., S. E. Schwartz, J. M. Hales, R. D. Cess, J. A. Coakley, Jr., J. E. Hansen, and D. J. Hofmann, 1992: Climate forcing by anthropogenic aerosols. *Science*, **255**, 423-430.

Han, Q., W. B. Rossow, and A. A. Lacis, 1994: Near-global survey of effective droplet radii in liquid water clouds using ISCCP data. *J. Climate*, **7**, 465-497.

Liu, Y. and P. H. Daum, 2000: Spectral dispersion of cloud droplet size distributions and the parameterization of cloud droplet effective radius. *Geophy. Res. Lett.*, **27**, 1903-1906.

Liu, Y. and J. Hallett, 1997: The "1/3" power-law between effective radius and liquid water content. *Quart. J. Roy. Meteor. Soc.*, **123**, 1789-1795.

Martin, G. M., D. W. Johnson, and A. Spice, 1994: The measurement and parameterization of effective radius of drops in warm stratocumulus clouds. *J. Atmos. Sci.*, **51**, 1823-1842.

Miles, N. L., J. Verlinde, and E. E. Clothiaux, 2000: Cloud droplet size distributions in low-level stratiform clouds. *J. Atmos. Sci.*, **57**, 295-311.

Twomey, S., M. Piepgrass, and T. L. Wolfe, 1984: An assessment of the impact of pollution on global cloud albedo. *Tellus*, **36B**, 356-366.